Published in final edited form as:
AJR Am J Roentgenol. 2008 December ; 191(6): . doi:10.2214/AJR.07.3693.

Molecular Breast Imaging: Use of a Dual-Head Dedicated Gamma Camera to Detect Small Breast Tumors

Carrie B. Hruska[1], **Stephen W. Phillips**[1], **Dana H. Whaley**[1], **Deborah J. Rhodes**[2], and **Michael K. O'Connor**[1]

[1]Department of Radiology, Mayo Clinic, 200 First St. SW, Rochester, MN 55905

[2]Department of Medicine, Mayo Clinic, Rochester, MN

Abstract

OBJECTIVE—Molecular breast imaging with a single-head cadmium zinc telluride (CZT) gamma camera has previously been shown to have good sensitivity for the detection of small lesions. To further improve sensitivity, we developed a dual-head molecular breast imaging system using two CZT detectors to simultaneously acquire opposing breast views and reduce lesion-to-detector distance. We determined the incremental gain in sensitivity of molecular breast imaging with dual detectors.

SUBJECTS AND METHODS—Patients with BI-RADS category 4 or 5 lesions < 2 cm that were identified on mammography or sonography and scheduled for biopsy underwent molecular breast imaging as follows: After injection of 740 MBq of technetium-99m (^{99m}Tc) sestamibi, 10-minute craniocaudal and mediolateral oblique views of each breast were acquired. Blinded reviews were performed using images from both detectors 1 and 2 and images from detector 1 only (simulating a single-head system). Lesions were scored on a scale of 1–5; 2 or higher was considered positive.

RESULTS—Of the 150 patients in the study, 128 cancers were confirmed in 88 patients. Averaging the results from the three blinded readers, the sensitivity of dual-head molecular breast imaging was 90% (115/128), whereas the sensitivity from review of only single-head molecular breast imaging was 80% (102/128). The sensitivity for the detection of cancers ≤ 10 mm in diameter was 82% (50/61) for dual-head molecular breast imaging and 68% (41/61) for single-head molecular breast imaging. On average, 13 additional cancers were seen on dual-head images and the tumor uptake score increased by 1 or more in 60% of the identified tumors.

CONCLUSION—Gains in sensitivity with the dual-head system molecular breast imaging are partially due to increased confidence in lesion detection. Molecular breast imaging can reliably detect breast lesions < 2 cm and dual-head molecular breast imaging can significantly increase sensitivity for subcentimeter lesions.

Keywords

breast cancer; breast neoplasms; gamma camera; mammography; molecular breast imaging; nuclear medicine

Address correspondence to C. B. Hruska (hruska.carrie@mayo.edu)..

GE Healthcare and Gamma Medica-Ideas provided the gamma cameras used in this project.

Mammography is the most widely used and most effective method for breast cancer screening; its implementation as a regular screening procedure has been shown to significantly decrease the breast cancer mortality rate [1-3]. However, because mammography is an anatomic imaging technique that uses low-energy x-rays to image differences in the radiographic density of tissue, the sensitivity of mammography can be significantly affected by fibroglandular tissue in the breast. For women who have radiographically dense breasts, the sensitivity of mammography is poor and has been reported to be less than 50% for women with an extremely dense pattern on mammograms [4]. This limitation of mammography is compounded by the fact that dense breast tissue is a significant risk factor for developing breast cancer [5, 6].

In an effort to overcome the known limitations of mammography, alternative breast imaging techniques are continually being studied. Digital mammography has been shown to provide a small but significant increase in sensitivity for the detection of breast cancer in the subgroup of women younger than 50 years who are pre- or perimenopausal and have dense breasts [7]; however, the benefits of digital mammography are debatable because of the failure of digital mammography to show any significant benefit in the general screening population [8-12] and because of its questionable cost-effectiveness at this time [13-15].

Considerable attention has been focused on imaging techniques such as sonography and MRI. The American College of Radiology Imaging Network (ACRIN) 6666 Trial compared whole-breast sonography and mammography and focused on women with radiographically dense breasts who also had a high risk of breast cancer. The initial results from that trial showed that the addition of screening sonography resulted in only a modest increase in cancer detected; among the 41 breast cancers detected in 2,637 women at high risk for breast cancer, 12 cancers were found by sonography alone (Berg WA et al., presented at the 2007 Radiological Society of North America meeting). However, sonography findings resulted in an additional 136 biopsies, giving it a biopsy rate of 5% compared with 2.6% for mammography. More problematic was the finding that the positive predictive value of sonography-prompted biopsies was only 8.5% compared with 29% for mammography.

The preliminary results from the ACRIN 6666 Trial are in line with those of several recent studies comparing mammography, sonography, and MRI for the detection of breast cancer [16-20]. These studies consistently show that both mammography and sonography have a low sensitivity for the detection of breast cancer in women at increased risk and report a sensitivity of between 75% and 100% for MRI. Partly as a result of these studies, the American Cancer Society recently recommended MRI as an adjunct to screening mammography in women at high risk [21]. However, the high cost of bilateral breast MRI (10–15 times that of mammography) and the large difference in specificity between tertiary care centers (≈ 90%) and community practice groups (≈ 50%) [21] may significantly limit the widespread use of this technology.

Nuclear medicine methods for breast imaging have existed since the early 1990s, when it was discovered that the radiotracer technetium-99m (^{99m}Tc) sestamibi can be used to image breast tumors with a technique called “scintimammography.” Because this technique is not influenced by breast density [22], it was thought to be particularly useful in women with dense breast parenchyma. However, because of poor spatial resolution and breast positioning limitations of conventional gamma cameras, this technique had poor sensitivity (< 50%) for the detection of small breast cancers (≤ 10 mm in diameter) [23, 24]. This limitation is particularly important in light of the fact that up to 30% of breast cancers detected on screening mammography [25] and 50% of those detected on MRI in screening studies [20] are smaller than 10 mm and explains the limited diagnostic value of scintimammography.

Advances in nuclear medicine technology over the past decade, both in the field of single-photon and positron emission detectors, have yielded various designs of small-field-of-view detectors dedicated for breast imaging [26-34]. The dedicated technologies offer significant improvements in both spatial and energy resolution and allow the breast to be positioned directly on the detector, permitting better detection of small breast tumors. In our laboratory we have developed the technique of molecular breast imaging that uses dedicated, small-field-of-view gamma cameras composed of the semiconductor cadmium zinc telluride (CZT) for single-photon planar imaging of the lightly compressed breast [35-37]. The solid-state CZT technology offers a factor of 2 or more improvement in both energy and spatial resolution, and its pixilated design extends the active field of view to within millimeters of the detector edge, permitting the breast to be placed directly on the detector and imaged in a manner similar to mammography [32].

Preliminary results from our laboratory and others indicate that molecular breast imaging has a potential role in a variety of both screening and diagnostic settings [35-46]. However, a critical requirement for any future role of molecular breast imaging in breast cancer detection is establishing the ability of molecular breast imaging to reliably detect small breast tumors (≤ 10 mm). Using a system composed of a single CZT gamma camera mounted on a modified mammography gantry, we previously showed that molecular breast imaging has an overall sensitivity of 74% for the detection of breast lesions smaller than 10 mm [37]. The results of this study showed that false-negative studies were strongly correlated with cases in which the lesion diameter was very small (≤ 5 mm), the compressed breast thickness was large (> 5 cm), and the count density in the images was lower than the median clinically observed value.

To increase the ability of molecular breast imaging to detect breast lesions that are small and lesions in women with large breasts or low uptake of radiotracer, we developed a dual-head dedicated gamma camera system to enable simultaneous acquisition of opposing views of the breast. The dual-head system allows simultaneous acquisition of superior and inferior views of the breast in the craniocaudal (CC) position and medial and lateral views in the mediolateral oblique (MLO) position.

The objective of this study was to determine the incremental gain in sensitivity of molecular breast imaging for the detection of small breast lesions with the additional views provided by a dual-detector system.

Subjects and Methods

Research Plan

Molecular breast imaging was performed in patients with suspicious breast lesions identified on mammography or sonography before biopsy of the lesion. The molecular breast imaging examinations were read in a blinded fashion, first using the detector 1 images only to simulate single-head molecular breast imaging data, and then using the complete dual-head data from both detectors 1 and 2. Results were then compared to determine gains in sensitivity with the addition of a second detector head. Pathology results were used as the reference standard.

Instrumentation for Molecular Breast Imaging

Three slightly different prototype dual-head gamma camera systems were used in this study because the technology was undergoing development concurrently with the study. Each system was configured with two opposing small-field-of-view CZT detectors that were mounted on a modified mammography gantry as shown in Figure 1. The single-head system used previously in our laboratory [35-37] was similar in design, but used only detector 1,

which was typically used to image the breast from the inferior and lateral sides in CC and MLO positions, respectively. Detector 2 was added to construct the dual-head system, permitting the breast to be imaged from the superior side in CC views and the medial side in MLO views at the same time as the corresponding detector 1 views.

The detectors used in the dual-head systems were either prototype CZT detectors (GE Healthcare) or LumaGem 3200s detectors (Gamma Medica-Ideas), which have been previously described in detail [32, 47, 48]. The prototype CZT detector comprised an 80 × 80 array of CZT elements with a pixel size of 2.5 × 2.5 mm, giving a total detector area of 20 × 20 cm. The LumaGem detector comprised a 96 × 128 array of CZT elements with a pixel size of 1.6 × 1.6 mm, giving a total detector area of 15 × 20 cm. Both detector types were fitted with high-sensitivity collimators, giving system sensitivities of 8.65 and 10.7 counts/ min/kBq (320 and 396 counts/min/μCi, respectively) for the prototype CZT and LumaGem systems, respectively.

From previous phantom studies, the use of high-sensitivity collimation was determined to be optimal for these dedicated breast imaging systems [48]. The first dual-head configuration comprised a LumaGem detector as detector 1 and a prototype CZT detector as detector 2. The second system comprised two prototype CZT detectors and the third system comprised two LumaGem detectors. Of 150 studies performed on the three systems, 66 were performed on the first system, six were performed on the second system, and the majority of studies (*n* = 78) were performed on the third prototype system.

Subjects

The protocol for this study was reviewed and approved by the institutional review board and written informed consent was obtained from all study participants. The criteria required for patient participation in the study were identical to those in our previous study examining the sensitivity of molecular breast imaging with a single CZT detector [37]. Briefly, patients selected for the study had a breast lesion that, first, was considered suspicious or highly suggestive of malignancy according to the BI-RADS atlas [49] criteria; second, was identified on mammography or sonography as being less than 2 cm in diameter; and, third, was scheduled for biopsy. Preference was given to patients who had lesions with a high likelihood of malignancy or that were suspicious for multifocal or multicentric disease.

Molecular Breast Imaging Procedure

Molecular breast imaging was performed before biopsy. Patients were injected with 740 MBq (20 mCi) of ^{99m}Tc sestamibi and each breast was imaged with one of the dual-head molecular breast imaging system configurations described earlier in both CC and MLO positions for 10 minutes per view. Nuclear medicine technologists who were trained in mammographic techniques positioned the breast for each study. The breast was positioned such that during CC views, detector 1 was located on the inferior side and detector 2 on the superior side of the breast; during MLO views, detector 1 was located on the lateral side and detector 2 on the medial side of the breast. For each image, the breast was lightly compressed between the two detector heads using a compression of 15-lb force. The thickness of the compressed breast was recorded for each molecular breast imaging view, and a measure of count density was obtained from region-of-interest analysis in an area of uniform uptake on molecular breast imaging.

On completion of each molecular breast imaging study, the images were reviewed in conjunction with images obtained from mammography, sonography, and occasionally MRI. In cases in which additional breast lesions were found on molecular breast imaging that were not seen on mammography or sonography, additional diagnostic examinations

(mammography, sonography, MRI, or a combination of these examinations) were performed as necessary to evaluate these lesions.

Data Analysis

The final histopathology of each lesion was obtained from surgical excision or core needle biopsy. For cases in which additional lesions were detected on molecular breast imaging and biopsy was not deemed necessary after additional diagnostic imaging, the interpretation of the subsequent annual screening mammograms and other imaging (including mammography, sonography, and MRI) and clinical findings during a 15-month follow-up period were used to verify the status of the lesions.

On completion of the 150 patient studies, all molecular breast images were again read by three radiologists independent of ancillary patient information or mammographic, sonographic, or MR images and in a blinded fashion. Briefly, a display program was written that removed patient-identifying information and randomized the order in which patient studies were displayed. In addition, for a given reading session, the program was configured to display either images from detector 1 only, simulating a single-head system, or images from both detectors 1 and 2, simulating a dual-head system. Radiologists read detector 1 images or images from both detector heads during separate reading sessions separated by at least 1 week without reference to their previous interpretation from the other molecular breast imaging session.

The distribution of radiotracer in the breast was assessed on molecular breast imaging; if the distribution was entirely uniform, was regionally photopenic, or exhibited normal physiologic non-mass-like radiotracer uptake, an uptake score of 1, indicating no focal uptake, was given. If abnormal focal uptake was observed, the radiologists electronically marked the location and intensity of abnormal radiotracer uptake on both the CC and MLO views. Lesions were given an uptake score on a scale from 2 to 5, with 2 meaning mild focal uptake; 3, moderate focal uptake; 4, strong focal uptake; and 5, intense focal uptake. The uptake score was also used as an indicator of the reader’s confidence in identifying each lesion.

For the assessment of sensitivity, lesions scored 2 or higher were considered positive. The McNemar test for correlated proportions was used to assess the statistical significance of cancers detected with the reading of detector 1 images only (single head) and cancer detected when the views from both detectors 1 and 2 (dual head) were available. The change in uptake score between interpretation of the single-head images and the dual-head images was calculated to determine if the addition of detector 2 altered the number of perceived lesions and their apparent intensity. The location of each lesion relative to detectors 1 and 2 was determined from mammography, sonography, or pathology reports to assess the impact of lesion location on the sensitivity of single- and dual-head molecular breast imaging.

Results

Subjects

A total of 150 patients participated in the study. Complete pathology results were obtained for 149 of these patients, and the remaining patient was lost to follow-up because she elected to not undergo surgery. In the 149 patients, a total of 245 lesions were evaluated. The histopathology of 235 lesions was determined from biopsy or surgical excision; in the remaining 10 lesions, positive findings were determined only on molecular breast imaging, and subsequent diagnostic imaging did not require biopsy; therefore, the 15-month follow-up analysis was used to establish the status of these 10 lesions.

The patients ranged in age from 25 to 92 years with a mean age of 59 years. Mammographic breast density was known in 138 of the 150 patients. Of these, 65 patients had > 50% breast density, including 54 with a heterogeneously dense breast pattern and 11 with an extremely dense breast pattern on mammography, and 73 patients had < 50% breast density. In the remaining 12 patients with unknown mammographic breast density, either mammography was not performed (i.e., lesion was detected on sonography) or mammography was performed at an outside institution.

The BI-RADS assessment of lesions was category 5 in approximately 50% of patients and category 4 in the other 50% of patients.

Breast Cancers

In the 149 patients in whom complete follow-up was available, 128 lesions were confirmed as cancer in 88 patients. Table 1 shows the distribution of tumor type and the sensitivity for each type. Approximately 70% of all cancers were either invasive ductal carcinoma (IDC), ductal carcinoma in situ (DCIS), or a combination of the two. Invasive lobular carcinoma (ILC) comprised the majority of the remaining cancers. Two tubular carcinomas, one medullary carcinoma, one metaplastic carcinoma, and one malignant phyllodes tumor were present.

Sensitivity of Molecular Breast Imaging

Blinded review of the dual-head molecular breast imaging studies detected an average of 115 of the 128 cancers for an average overall sensitivity of 90%. Agreement was excellent among the three blinded readings with 117, 117, and 111 tumors detected by the three reviewers. Table 2 shows the distribution of the sizes of the tumors in the study. The average tumor diameter was 13 ± 9 mm (± SD). The smallest breast tumor detected on molecular breast imaging was an IDC that was 3 mm in diameter and the largest tumor was a DCIS that extended over an area of 50 mm.

Also in Table 2, the sensitivity of molecular breast imaging as a function of breast tumor size and the number of detector heads used for interpretation are given for each blinded reader and as an average of the three readers. The sensitivity of dual-head molecular breast imaging for lesions ≤ 10 mm in diameter showed the greatest variation among the three blinded reviewers and was 85% (52/61), 85% (52/61), and 75% (46/61), respectively. Equivalent results for lesions ≤ 10 mm in diameter for single-head molecular breast imaging (detector 1 only) were 62% (38/61), 75% (46/61), and 66% (40/61). Sensitivity improved with tumor size, and all but two of 67 tumors greater than 10 mm in diameter were detected.

Figure 2 compares the sensitivity of single-head and dual-head molecular breast imaging in this study with previous results obtained with conventional scintimammography [50] as a function of tumor size. The sensitivity of molecular breast imaging for the smallest breast tumors (diameters ≤ 5 mm) increased from an average of 44% to 67% with the addition of the second detector head. Although the gain in sensitivity with dual-head molecular breast imaging over single-head molecular breast imaging was not statistically significant for each subset of tumor diameters shown in Table 2, the overall gain in sensitivity for all tumor sizes with the addition of detector 2 was highly significant ($p < 0.0005$).

The sensitivity of molecular breast imaging did not appear to be greatly affected by changes in the detector configuration throughout the study. The average sensitivity obtained with the first dual-head configuration (LumaGem detector as detector 1 and prototype CZT detector as detector 2) was 92% (55/60). Only three tumors, all larger than 13 mm, were imaged with the second configuration (two prototype CZT detectors), and all three were detected. The

average sensitivity of the third system (two LumaGem detectors) was 88% (57/65). The average tumor diameters imaged with the first and third configurations were similar at 13.4 and 13.3 mm, respectively.

Nine cancers in eight patients were false-negative on molecular breast imaging by all three blinded readers. A summary of these false-negative tumors is given in Table 3. The false-negative cancers were predominantly small. Four of the false-negatives were tumors with diameters ≤ 5 mm and seven were < 8 mm. Two false-negatives were thought to be due to inadequate patient positioning: One patient was severely kyphotic (tumor 1 in Table 3) and another was obese (tumor 7 in Table 3), making positioning difficult in these cases. In addition, in one patient (tumors 3a and 3b in Table 3), a high level of bilateral non-mass-like uptake of the radiotracer was present that may have obscured two small tumors in the molecular breast images of that patient. This non-mass-like uptake may have been related to increased hormonal activity in the breast because this patient was a user of estrogen therapy for the treatment of postmenopausal symptoms.

In 12 patients, 12 additional breast cancers were found on molecular breast imaging that were occult on mammography and sonography: 11 of these cancers were additional foci to the index lesion detected with mammography, and one cancer was the index lesion. In the latter case, the original lesion identified on mammography was a grossly enlarged lymph node that was highly suspicious for malignancy. In these 12 patients, four had heterogeneously dense breasts on mammography and six had scattered fibroglandular densities; in the other two patients, breast density was not known. All 12 cancers were detected on additional imaging (second-look mammography, sonography, or MRI) and were confirmed as true cancer at biopsy. These cancers included three cases of IDC, three cases of ILC, one case of mixed IDC and ILC, and five cases of DCIS.

The incremental gain in sensitivity of a dual-head system over a single-head system was assessed by comparing uptake scores assigned to each tumor in each view. As shown in Table 2, of the 128 tumors identified in the blinded review, an average of 102 tumors (range, 98–108 tumors) were identified from the single-head (detector 1) images, and on average an additional 13 tumors (range, 9–19 tumors) were identified with the addition of detector 2 images during interpretation. Table 4 displays the sensitivity of single-head and dual-head molecular breast imaging according to the location of the tumor within the breast. The most frequent location of tumors was the upper outer quadrant of the breast. For all locations, the sensitivity was increased with dual-head molecular breast imaging, although the individual increases for each location were not statistically significant. The greatest increase in absolute sensitivity was observed for tumors in the upper inner quadrant; in that area, sensitivity increased from 74% with single-head molecular breast imaging to 91% when dual-head images were used.

The tumor uptake score increased in either one or both of the CC or MLO views with the addition of the detector 2 images in 60% of the tumors (208/345) identified by the three reviewers; the uptake score decreased in either the CC or MLO view for 15% of the tumors (53/345) and remained unchanged in both CC and MLO views in 26% (91/345). This increase in uptake score for the majority of tumors indicates increased confidence in lesion detection with the addition of the detector 2 views.

Figures 3-5 illustrate cases in which either lesions were seen clearly only on the additional views provided by detector 2, or the addition of the opposing detector 2 views was important in increasing the confidence of the radiologist in image interpretation. Figure 3 shows a medially located IDC detected only on the upper MLO view. Figure 4 illustrates a study in which the primary tumor was identified on the detector 1 views, but an adjacent area of

DCIS was identified only on the detector 2 superior CC image. Figure 5 presents a study in which a 4-mm cancer in the upper mid breast was not diagnosed with the detector 1 views, but it was detected when all the dual-head views from both detectors were available.

In addition to determining the value of a second detector head, we also assessed the value of each view in achieving the overall sensitivity of molecular breast imaging. Results presented in Table 5 show that no single view was able to detect all lesions and that both CC and MLO views with a dual-detector configuration were necessary to achieve the highest sensitivity.

Breast Thickness and Count Density on Molecular Breast Imaging

The range of compressed breast thicknesses in CC views was 3.0–11.5 cm with a mean and SD of 6.6 ± 1.4 cm. In MLO views, breast thickness ranged between 3.1 and 11.0 cm with a mean and SD of 6.7 ± 1.4 cm. The sensitivity of dual-head molecular breast imaging did not appear to be affected by breast thickness. As shown in Table 3, in the six patients with adequate positioning, there were seven false-negatives. Five of these undetected tumors were in patients with compressed breast thicknesses between 6 and 7.5 cm, which is within 1 SD of the mean thickness. In 51 patients with increased breast thickness (> 7.5 cm), sensitivity was more than 93% for all three readers. The median count density was 118 counts/cm^2/min/kBq, and the 10th and 90th percentile values were 68 and 191 counts/cm^2/min/kBq, respectively. Four of the false-negative cases in Table 3 (tumors 2, 4, 5, and 6) occurred in patients with lower count densities—that is, count densities lower than the 20th percentile.

Benign Lesions

In addition to the 128 cancers, 117 benign breast lesions were identified on mammography, sonography, or molecular breast imaging in 85 patients. False-positive findings from mammography or sonography (or both) occurred in 107 benign lesions in 77 patients. Molecular breast imaging yielded false-positive findings in 42 breast lesions in 38 patients.

Biopsy or surgical excision was performed in 32 of the 42 breast lesions that were false-positive on molecular breast imaging; the histopathology of those lesions was fibroadenoma (*n* = 10), papilloma (*n* = 5), fat necrosis (*n* = 2), stromal fibrosis (*n* = 2), sclerosing adenosis (*n* = 2), benign lymph node (*n* = 1), benign phyllodes tumor (*n* = 1), radial scar (*n* = 1), atypical papilloma (*n* = 1), atypical lobular hyperplasia (*n* = 1), atypical ductal hyperplasia (*n* = 3), and benign breast tissue (*n* = 3). The 10 other false-positive breast lesions on molecular breast imaging were not detected on the initial mammography or sonography examinations, and biopsy was not performed because of negative or benign findings on subsequent diagnostic imaging studies performed to evaluate these lesions. For all 10 lesions, the 15-month follow-up analysis verified the lesions to be benign. The average molecular breast imaging uptake score of the false-positives was 2 in 18 lesions, 3 in 13 lesions, 4 in nine lesions, and 5 in two lesions. Of the 11 breast lesions with an uptake score of 4 or higher, six were fibroadenomas, three were papillomas, one was a papilloma with atypia, and one was sclerosing fat necrosis.

Specificity of Molecular Breast Imaging

Benign pathology results on biopsy indicated that 61 patients did not have breast cancer. Molecular breast imaging findings were true-negative for 41, 42, and 43 patients in the three blinded reviews, respectively, giving an average specificity of 69% (42/61). We should note, however, that because all patients in this study were required to have a mammographically suspicious lesion, this specificity does not necessarily reflect the specificity of molecular breast imaging in a screening population.

Discussion

A new molecular breast imaging system comprising dual-head CZT detectors was developed and its ability to detect lesions < 2 cm in diameter was evaluated. The results of this study showed that the use of dual-head CZT detectors can increase the sensitivity of molecular breast imaging for the detection of small breast lesions. Sensitivity was significantly increased from 80% to 90% ($p < 0.0005$) for all 128 breast tumors in the study with the use of views from dual-head molecular breast imaging rather than views from a single-head system (detector 1 only) for interpretation. Results obtained with single-head molecular breast imaging showed an average sensitivity of 68% for the detection of breast tumors ≤ 10 mm in diameter. This sensitivity is similar to that previously reported for a single-head system [37]. The use of a dual-head system resulted in a significant increase in the sensitivity—from 68% to 82%—for the detection of tumors ≤ 10 mm in diameter ($p = 0.004$). The greatest improvements in absolute sensitivity with the dual-head system over a single-head configuration were the increase in sensitivity from 44% to 67% for the smallest tumors with diameters ≤ 5 mm and the increase in sensitivity from 74% to 91% for tumors located in the upper inner quadrant of the breast, although these differences were not statistically significant because of small sample sizes.

A limitation of this study is that it was not designed to compare molecular breast imaging with standard diagnostic mammography and sonography. The goal of this study was to determine whether molecular breast imaging can detect small breast lesions and whether the additional views from a second detector head can increase the sensitivity of molecular breast imaging for the detection of breast cancer. Mammography, sonography, or both were used to initially identify the small breast lesions, and lesions were specifically selected to ensure a high likelihood of breast cancer. To compare the single-head molecular breast imaging results with dual-head results and achieve statistical significance, we needed to study a large number of small cancers. Although molecular breast imaging did detect additional breast cancers that were occult on mammography, we anticipate that molecular breast imaging will now be useful as an adjunct technique, especially in women who are not served well by mammography, such as those with dense breasts. We are currently conducting a large screening trial at our institution to evaluate the use of molecular breast imaging in women who have mammographically dense breasts and an increased risk for breast cancer.

To our knowledge, this study is the first clinical study conducted using a dual-head configuration of a molecular breast imaging system and is the largest study, in terms of the number of tumors and patients studied, performed to date evaluating the sensitivity of molecular breast imaging in a diagnostic setting. During the past decade, several other laboratories have reported results from small clinical studies performed using dedicated single-head systems. Using single detectors comprising pixilated arrays of CsI and NaI, respectively, for their studies, both Maini et al. [38] and Brem et al. [40] reported sensitivities for tumors ≤ 10 mm of 67%, closely agreeing with the sensitivity reported in this study for the interpretation of only single-head views. In another early study, Scopinaro and colleagues [39] obtained a high sensitivity of 81% for tumors ≤ 10 mm using a single-head prototype CsI detector. Most recently, Spanu et al. [45] reported a remarkable 90% sensitivity for cancers ≤ 10 mm using the radiotracer ^{99m}Tc tetrofosmin and a single CZT detector identical to the detectors used in our dual-head system.

Although the sensitivities reported by Scopinaro and colleagues [39] and Spanu and colleagues [45] for tumors ≤ 10 mm with single-head systems were close to or better than the 82% sensitivity we report here with dual-head CZT detectors, key differences in the studies may explain this discrepancy. One factor to be considered is the method used for interpreting the images. While all studies discussed here [38-40, 45] used a blinded

interpretation of the dedicated gamma camera images, the studies from other laboratories relied on a consensus reading whenever individual readers disagreed, whereas in this study, readers independently interpreted the images and the reported sensitivity was an average of their individual results. If a consensus reading had been performed, we would have expected the only false-negatives to be those that were undiagnosed by all three readers (given in Table 3), and theoretically, sensitivity would have improved to 93% overall and 89% for the detection of tumors ≤ 10 mm for the dual-head molecular breast imaging system.

Because of this difference in interpretation methods and a variety of other differences among the studies examining the sensitivity of molecular breast imaging, including considerable differences in detector technologies, radiotracers, breast compression, and so on, it is difficult to directly compare the results presented here with those from other laboratories. Regardless of absolute differences in reported sensitivities, it is clear from our work and that of other researchers that breast imaging with dedicated gamma cameras offers sensitivity for the detection of breast cancer that is superior to that reported for conventional scintimammography [23, 24] and offers a high sensitivity for cancers ≤ 10 mm. In this study, sensitivities from single-head and dual-head molecular breast imaging systems were compared directly by simulating both types of acquisitions in each patient; the results showed that dual-head molecular breast imaging significantly improves both overall sensitivity and sensitivity for the detection of breast tumors ≤ 10 mm.

Several factors contributed to this increase in sensitivity. The addition of a second opposing detector head essentially decreases the maximum distance between the lesions and either detector to half the total compressed breast thickness. Simulations in our laboratory have shown that the ability to detect lesions ≤ 10 mm decreases sharply as the distance from the lesion to the detector face increases beyond 5 cm [48]. A previous study from our laboratory showed that many false-negative studies occurred in patients with breast thicknesses greater than 5 cm [37]. Despite an increase in the average compressed breast thickness in CC views from 5.3 ± 1.4 cm in the previous study to 6.6 ± 1.4 cm in this study, breast thickness was not a major factor contributing to false-negatives with the dual-head system. With the use of opposing heads, the maximum possible lesion-to-detector distance in this study would have been 5.75 cm (half the maximum breast thickness of 11.5 cm), which is significantly less than the maximum breast thickness of 9 cm obtained in the single-head study.

The provision of superior and medial views of the breast in addition to inferior and lateral views not only increased sensitivity but also increased the confidence of the blinded reviewers in identifying lesions, as evidenced by an increase in uptake score in 60% of tumors with the addition of upper head views. Thus we believe that acquiring both views from both detectors 1 and 2 provides important additional information that aids in reading the molecular breast imaging examinations and detecting very faint breast lesions. For example, Figure 4 shows faint lesions in the detector 1 views that appear much more clearly in the detector 2 views.

The use of a dual-head system is not absolutely necessary for acquiring opposing views of the breast because it is possible to obtain the superior and inferior views of the CC position and medial and lateral views of the MLO position with separate acquisitions performed using only a single-head detector. However, acquiring the views in that fashion would require additional repositioning of the breast on the camera and would double the imaging time for bilateral molecular breast imaging from 40 to 80 minutes. In our experience of performing molecular breast imaging in more than 1,400 patients, we believe that 40 minutes is already nearing the limit of patient tolerance for remaining upright and still throughout the molecular breast imaging procedure. The dual-head system thus offers the ability to acquire simultaneous opposing views of the breast, while maintaining identical

breast positioning and compression for each of the opposing views, and does not require additional imaging time. We realize that the cost of the molecular breast imaging system would be increased by adding a second detector head; however, because this study was a preliminary study with a prototype system, a true cost-benefit ratio of commercial dual-head molecular breast imaging compared with single-head molecular breast imaging is yet to be determined.

We previously reported that the count density in 10-minute molecular breast images acquired with ^{99m}Tc sestamibi was generally low when a high-resolution collimator was used [37]. All false-negative studies in our previous study occurred in patients in which count density was at or below the median value of 41 counts/cm^2/min/kBq with a high-resolution collimator. The use of high-sensitivity collimators in the dual-head system increased the median count density by nearly a factor of 3 to 118 counts/cm^2/min/kBq. Although this increase in sensitivity comes with a slight loss of resolution with depth, this loss is offset by the use of opposing detectors so that the maximum distance of a lesion from the collimator face is never greater than half the breast thickness. With the use of this high-sensitivity collimator for low-count breast imaging, it was found that count density was no longer a significant factor contributing to negative studies. Of the four false-negative studies occurring in patients with low count densities, the count densities were between 64 and 74 counts/cm^2/min/kBq, which is still a factor of 1.5 greater than the median value obtained in our previous study [37].

One important change between our previous study and this study was the use of nuclear medicine technologists who have been properly trained in mammographic techniques to ensure correct breast positioning for the molecular breast imaging examinations. In our previous study, the nuclear medicine technologists had little or no experience in breast positioning and performed all examinations unaided. We believe that all molecular breast imaging studies should be performed by technologists who are adequately trained in good mammographic breast positioning techniques. In the previous study, at least five of the 10 false-negative cancers were believed to be outside the detector field of view because of inadequate breast positioning. In this study, two of nine cancers that were false-negative by all reviewers were not within the field of view and in both cases suboptimal positioning was due to patient factors (obesity, kyphosis) rather than poor technique on the part of the technologists.

Another potential benefit of the dual-head system is the ability to perform quantitative lesion analysis and image enhancement using opposing detector views and knowledge of breast thickness. Methods to quantitate lesion size, the depth of the lesion from the detector, and uptake of the radiotracer are currently under investigation in our laboratory [51]. The use of two opposing detectors enables the creation of a geometric mean image that, combined with knowledge of breast thickness, permits the application of resolution-recovery techniques much like those currently used in SPECT [52]. Application of these techniques may permit the use of a reduced acquisition time or, conversely, a reduction in the administered dose of ^{99m}Tc sestamibi.

The ability to obtain quantitative information from the geometric mean image should also enable this technology to be used to quantitate absolute tumor uptake and changes in tumor function. Measurement of absolute tumor uptake of ^{99m}Tc sestamibi may enable better discrimination between benign and malignant processes in the breast. In addition, the ability to quantitate changes in uptake may have potential application in monitoring the response to neoadjuvant therapy.

The quantitative potential of molecular breast imaging aside, we believe that the results presented here indicate that molecular breast imaging has overcome the limitations of scintimammography for the detection of small breast tumors and warrants further exploration as a valuable clinical tool on a par with conventional diagnostic imaging techniques such as mammography, sonography, and MRI. The results from this study have shown that sestamibi is a significantly better radiopharmaceutical for tumor imaging in the breast than previously believed and that the failure to recognize its potential value was in a major part because of inadequate technology. With the commercial development of dedicated breast imaging systems, we believe that additional radiopharmaceuticals may prove to be better than or complementary to sestamibi in the evaluation of breast pathology, thereby allowing a significant expansion of the field of molecular breast imaging.

Acknowledgments

We are grateful to study coordinators Margaret Drews-Radke and Barb Siem and nuclear medicine technologists Torey Alabin and Michelle Bartel for their work on this study.

This study was supported in part by funding from the National Cancer Institute under grant CA 110162.

C. B. Hruska and M. K. O'Connor have filed a patent on quantitation methods of dual-head molecular breast imaging. M. K. O'Connor is also principal investigator on a research grant awarded by the National Institutes of Health to the Mayo Clinic and Gamma Medica-Ideas.

References

1. Fletcher SW, Elmore JG. Clinical practice: mammographic screening for breast cancer. N Engl J Med. 2003; 348:1672–1680. [PubMed: 12711743]
2. Kerlikowske K, Grady D, Rubin SM, Sandrock C, Ernster VL. Efficacy of screening mammography: a meta-analysis. JAMA. 1995; 273:149–154. [PubMed: 7799496]
3. Tabar L, Vitak B, Chen HH, Yen MF, Duffy SW, Smith RA. Beyond randomized controlled trials: organized mammographic screening substantially reduces breast carcinoma mortality. Cancer. 2001; 91:1724–1731. [PubMed: 11335897]
4. Kolb TM, Lichy J, Newhouse JH. Comparison of the performance of screening mammography, physical examination, and breast US and evaluation of factors that influence them: an analysis of 27,825 patient evaluations. Radiology. 2002; 225:165–175. [PubMed: 12355001]
5. Boyd NF, Guo H, Martin LJ, et al. Mammographic density and the risk and detection of breast cancer. N Engl J Med. 2007; 356:227–236. [PubMed: 17229950]
6. Buist DSM, Porter PL, Lehman C, Taplin SH, White E. Factors contributing to mammography failure in women aged 40–49 years. J Natl Cancer Inst. 2004; 96:1432–1440. [PubMed: 15467032]
7. Pisano ED, Hendrick RE, Yaffe MJ, et al. Diagnostic accuracy of digital versus film mammography: exploratory analysis of selected population subgroups in DMIST. Radiology. 2008; 246:376–383. [PubMed: 18227537]
8. Pisano ED, Gatsonis C, Hendrick E, et al. Digital Mammographic Imaging Screening Trial (DMIST) Investigators Group. Diagnostic performance of digital versus film mammography for breast-cancer screening. N Engl J Med. 2005; 353:1773–1783. erratum in *N Engl J Med* 2006; 355:1840. [PubMed: 16169887]
9. Lewin JM, Hendrick RE, D'Orsi CJ, et al. Comparison of full-field digital mammography with screen-film mammography for cancer detection: results of 4,945 paired examinations. Radiology. 2001; 218:873–880. [PubMed: 11230669]
10. Lewin JM, D'Orsi CJ, Hendrick RE, et al. Clinical comparison of full-field digital mammography and screen-film mammography for detection of breast cancer. AJR. 2002; 179:671–677. [PubMed: 12185042]
11. Skaane P, Young K, Skjennald A. Population-based mammography screening: comparison of screen-film and full-field digital mammography with soft-copy reading—Oslo I study. Radiology. 2003; 229:877–884. [PubMed: 14576447]

12. Skaane P, Skjennald A. Screen-film mammography versus full-field digital mammography with soft-copy reading: randomized trial in a population-based screening program—the Oslo II study. Radiology. 2004; 232:197–204. [PubMed: 15155893]
13. Yaffe MJ, Barnes GT, Orton CG. Point/counterpoint: film mammography for breast cancer screening in younger women is no longer appropriate because of the demonstrated superiority of digital mammography for this age group. Med Phys. 2006; 33:3979–3982. [PubMed: 17153375]
14. Dershaw DD. Film or digital mammographic screening? N Engl J Med. 2005; 353:1846–1847. [PubMed: 16251541]
15. Tosteson ANA, Stout NK, Fryback DG, et al. Cost-effectiveness of digital mammography breast cancer screening. Ann Intern Med. 2008; 148:1–10. [PubMed: 18166758]
16. Kuhl CK, Schmutzler RK, Leutner CC, et al. Breast MR imaging screening in 192 women proved or suspected to be carriers of a breast cancer susceptibility gene: preliminary results. Radiology. 2000; 215:267–279. [PubMed: 10751498]
17. Warner E, Plewes DB, Hill KA, et al. Surveillance of *BRCA1* and *BRCA2* mutation carriers with magnetic resonance imaging, ultrasound, mammography and clinical breast examination. JAMA. 2004; 292:1317–1325. [PubMed: 15367553]
18. Kriege M, Brekelmans CT, Boetes C, et al. Efficacy of MRI and mammography for breast-cancer screening in women with a familial or genetic pre-disposition. N Engl J Med. 2004; 351:427–437. [PubMed: 15282350]
19. Leach MO, Boggis CR, Dixon AK, et al. Screening with magnetic resonance imaging and mammography of a UK population at high familial risk of breast cancer: a prospective multicentre cohort study (MARIBS). Lancet. 2005; 365:1769–1778. [PubMed: 15910949]
20. Sardanelli F, Podo F. Breast MR imaging in women at high-risk of breast cancer: is something changing in early breast cancer detection? Eur Radiol. 2007; 17:873–887. [PubMed: 17008989]
21. Saslow D, Boetes C, Burke W, et al. American Cancer Society Breast Cancer Advisory Group. American Cancer Society guidelines for breast screening with MRI as an adjunct to mammography. CA Cancer J Clin. 2007; 57:75–89. erratum in *CA Cancer J Clin* 2007; 57:185. [PubMed: 17392385]
22. Khalkhali I, Baum JK, Villanueva-Meyer J, et al. (99m)Tc sestamibi breast imaging for the examination of patients with dense and fatty breasts: multicenter study. Radiology. 2002; 222:149–155. [PubMed: 11799940]
23. Taillefer R. The role of ^{99m}Tc-sestamibi and other conventional radiopharmaceuticals in breast cancer diagnosis. Semin Nucl Med. 1999; 29:16–40. [PubMed: 9990681]
24. Waxman AD. The role of (99m)Tc methoxyisobutylisonitrile in imaging breast cancer. Semin Nucl Med. 1997; 27:40–54. [PubMed: 9122723]
25. Smart CR, Byrne C, Smith RA, et al. Twenty-year follow-up of the breast cancers diagnosed during the Breast Cancer Detection Demonstration Project. CA Cancer J Clin. 1997; 47:134–149. [PubMed: 9152171]
26. Majewski S, Kieper D, Curran E, et al. Optimization of dedicated scintimammography procedure using detector prototypes and compressible phantoms. IEEE Trans Nucl Sci. 2001; 48:822–829.
27. McElroy DP, Hoffman EJ, MacDonald L, et al. Evaluation of breast tumor detectability with two dedicated, compact scintillation cameras. IEEE Trans Nucl Sci. 2002; 49:794–802.
28. Pani R, Soluri A, Scafe R, et al. Multi-PSPMT scintillation camera. IEEE Trans Nucl Sci. 1999; 46:702–708.
29. Gruber GJ, Moses WW, Derenzo SE, Wang NW, Beuville E, Ho MH. A discrete scintillation camera module using silicon photodiode readout of CsI(Tl) crystals for breast cancer imaging. IEEE Trans Nucl Sci. 1998; 45:1063–1068.
30. Patt BE, Iwanczyk JS, Rossington Tull C, Wang NW, Tornai MP, Hoffman EJ. High resolution CsI(Tl) / Si-PIN detector development for breast imaging. IEEE Trans Nucl Sci. 1998; 45:2126–2131.
31. Kim JH, Choi Y, Joo KS, et al. Development of a miniature scintillation camera using an NaI(Tl) scintillator and PSPMT for scintimammography. Phys Med Biol. 2000; 45:3481–3488. [PubMed: 11098918]

32. Mueller B, O'Connor MK, Blevis I, et al. Evaluation of a small CZT detector for scintimammography. J Nucl Med. 2003; 44:602–609. [PubMed: 12679406]
33. Abreu MC, Almeida P, Balau F, et al. Clear-PEM: a dedicated PET camera for improved breast cancer detection. Radiat Prot Dosimetry. 2005; 116(1–4 Pt 2):208–210. [PubMed: 16604628]
34. Smith MF, Raylman RR, Majewski S, Weisenberger AG. Positron emission mammography with tomographic acquisition using dual planar detectors: initial evaluations. Phys Med Biol. 2004; 49:2437–2452. [PubMed: 15248588]
35. O'Connor MK, Phillips SW, Rhodes DJ, Collins DA. Reliable detection of small breast tumors with Tc-99m sestamibi and a dedicated small field of view gamma camera. J Nucl Med. 2004; 45:357P. (abstr). [PubMed: 15001674]
36. Rhodes DJ, O'Connor MK, Phillips SW, Smith RL, Collins DA. Molecular breast imaging: a new technique using technetium Tc 99m scintimammography to detect small tumors of the breast. Mayo Clinic Proc. 2005; 80:24–30.
37. O'Connor MK, Phillips SW, Hruska CB, Rhodes DJ, Collins DA. Molecular breast imaging: advantages and limitations of a scintimammographic technique in patients with small breast tumors. Breast J. 2007; 13:3–11. [PubMed: 17214787]
38. Maini CL, de Notaristefani F, Tofani A, et al. ^{99m}Tc-MIBI scintimammography using a dedicated nuclear mammograph. J Nucl Med. 1999; 40:46–51. [PubMed: 9935055]
39. Scopinaro F, Pani R, de Vincentis G, Soluri A, Pellegrini R, Porfiri L. High resolution scintimammography improves the accuracy of Tc-99m methoxyisobutylisonitrile scintimammography: use of a new dedicated gamma camera. Eur J Nucl Med. 1999; 26:1279–1288. [PubMed: 10541826]
40. Brem RF, Schoonjans JM, Kieper DA, Majewski S, Goodman S, Civelek C. High-resolution scintimammography: a pilot study. J Nucl Med. 2002; 43:909–915. [PubMed: 12097461]
41. Coover LR, Caravaglia G, Kuhn P. Scintimammography with dedicated breast camera detects and localizes occult carcinoma. J Nucl Med. 2004; 45:553–558. [PubMed: 15073249]
42. Brem RF, Rapelyea JA, Zisman G, et al. Occult breast cancer: scintimammography with high-resolution breast-specific gamma camera in women at high risk for breast cancer. Radiology. 2005; 237:274–280. [PubMed: 16126919]
43. Brem RF, Petrovitch I, Rapelyea JA, Young H, Teal C, Kelly T. Breast-specific gamma imaging with ^{99m}Tc-sestamibi and magnetic resonance imaging in the diagnosis of breast cancer: a comparative study. Breast J. 2007; 13:465–469. [PubMed: 17760667]
44. Brem RF, Fishman M, Rapelyea JA. Detection of ductal carcinoma in situ with mammography, breast specific gamma imaging, and magnetic resonance imaging: a comparative study. Acad Radiol. 2007; 14:945–950. [PubMed: 17659240]
45. Spanu A, Cottu P, Manca A, Chessa F, Sanna D, Madeddu G. Scintimammography with dedicated breast camera in unifocal and multifocal/multicentric primary breast cancer detection: a comparative study with SPECT. Int J Oncol. 2007; 31:369–377. [PubMed: 17611694]
46. O'Connor MK, Rhodes DJ, Hruska CB, Phillips SW, Whaley DH. Molecular breast imaging (MBI) as an adjunct to screening mammography. J Nucl Med. 2008; 49:41P. (abstr).
47. O'Connor MK, Wagenaar DJ, Hruska CB, Phillips S, Caravaglia G, Rhodes D. Molecular breast imaging using a dedicated high-performance instrument. Optics and photonics 2006: Hard X-ray And Gamma-ray Detector Physics And Penetrating Radiation Systems VIII. Proc SPIE. 2006:63191D1–63191D14.
48. Hruska CB, O'Connor MK. Effect of collimator selection on tumor detection for dedicated nuclear breast imaging systems. IEEE Trans Nucl Sci. 2006; 53:2680–2689.
49. American College of Radiology. Illustrated breast imaging reporting and data system (BI-RADS) atlas. 4th ed. American College of Radiology; Reston, VA: 2003.
50. Palmedo H, Biersack HJ, Lastoria S, et al. Scintimammography with technetium-99m methoxyisobutylisonitrile: results of a prospective European multicentre trial. Eur J Nucl Med. 1998; 25:375–385. [PubMed: 9553167]
51. Hruska CB, O'Connor MK. Quantification of lesion size, depth, and uptake using a dual-head molecular breast imaging system. Med Phys. 2008; 35:1365–1376. [PubMed: 18491531]

52. van Elmbt L, Walrand S. Simultaneous correction of attenuation and distance-dependent resolution in SPECT: an analytical approach. Phys Med Biol. 1993; 38:1207–1217.

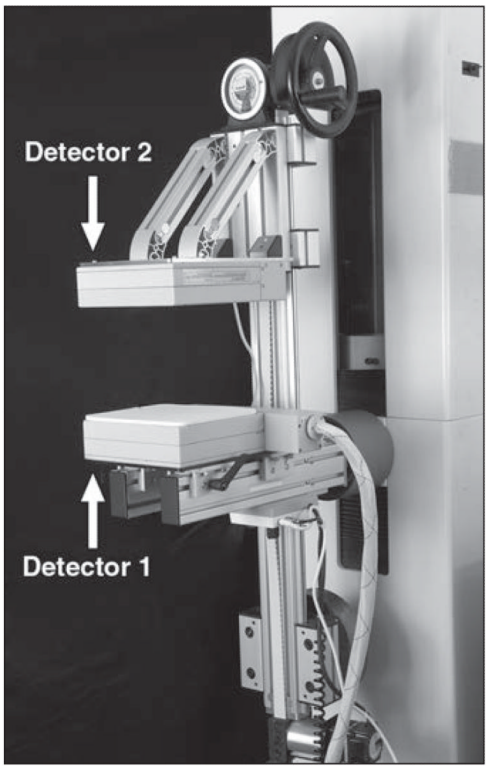

Fig. 1.
Photograph shows a dual-head molecular breast imaging system comprising two cadmium zinc telluride detectors mounted on modified mammographic gantry. To perform molecular breast imaging, the breast is lightly compressed between two detectors. When imaging the breast in craniocaudal position, detector 1 is located inferiorly and detector 2 is located superiorly to the breast. To image the breast in mediolateral oblique position, gantry is rotated so that detector 1 is located laterally and detector 2 is located medially to the breast.

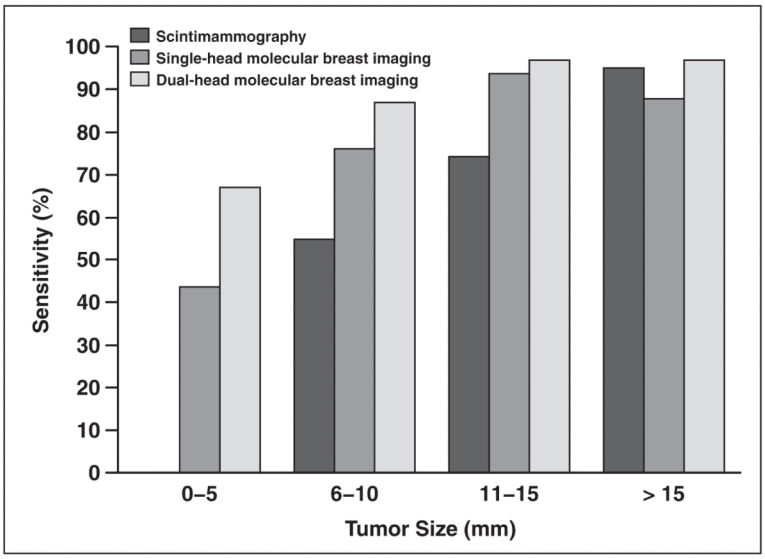

Fig. 2.

Bar graph shows sensitivity of molecular breast imaging for detection of breast tumors as function of tumor size. Results are shown for single-head molecular breast imaging system (lower detector), dual-head molecular breast imaging system, and scintimammography [49]. Note that no data were reported for detection of tumors 0–5 mm with scintimammography.

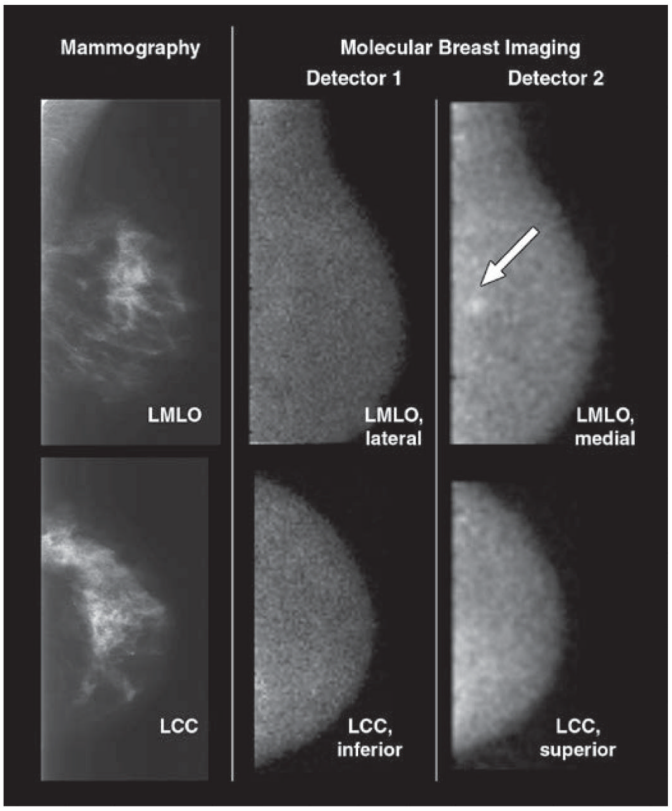

Fig. 3.

70-year-old woman with 6-mm invasive ductal carcinoma (*arrow*) in upper inner left breast initially identified on mammography as BI-RADS category 4 lesion. Screening mammograms and craniocaudal and mediolateral oblique views from both molecular breast imaging detectors are shown. When inferior and lateral molecular breast imaging views acquired with detector 1 (*middle images*) were reviewed in blinded reading session, they were interpreted as showing negative findings. When both inferior and lateral views from detector 1 and superior and medial molecular breast imaging views from detector 2 (*right images*) were available for interpretation, cancer was identified in medial view alone. Average uptake score of lesion visualized with molecular breast imaging was 3 (moderate focal uptake). LMLO = left mediolateral oblique, LCC = left craniocaudal.

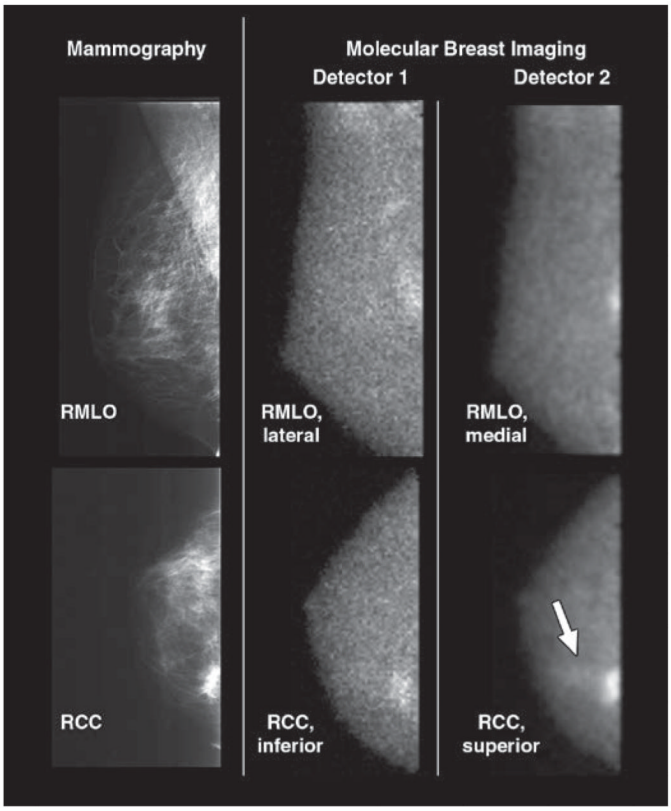

Fig. 4.

46-year-old woman with two foci of mixed invasive ductal carcinoma with ductal carcinoma in situ in upper inner right breast: One is located at 1-o'clock position 7 cm from nipple and second is located at 2-o'clock position 3 cm from nipple. Cancers were initially identified on mammography and sonography as BI-RADS category 5 lesions. Screening mammogram and craniocaudal and mediolateral oblique views from both molecular breast imaging detectors are shown. During blinded readings, when inferior and lateral molecular breast imaging views acquired with detector 1 (*middle images*) were available for interpretation (corresponding to views from single-head molecular breast imaging), one focus of cancer was detected. When superior and medial molecular breast imaging views from detector 2 were available in addition to detector 1 views during separate blinded reading session, same cancer was identified but average lesion uptake score was increased from 3 to 5, indicating increase in reader confidence in identifying lesion. Also, with additional detector 2 views, second focus of cancer (*arrow*) was identified as blush of low-intensity uptake (uptake score of 2) visible in superior craniocaudal view only. RMLO = right mediolateral oblique, RCC = right craniocaudal.

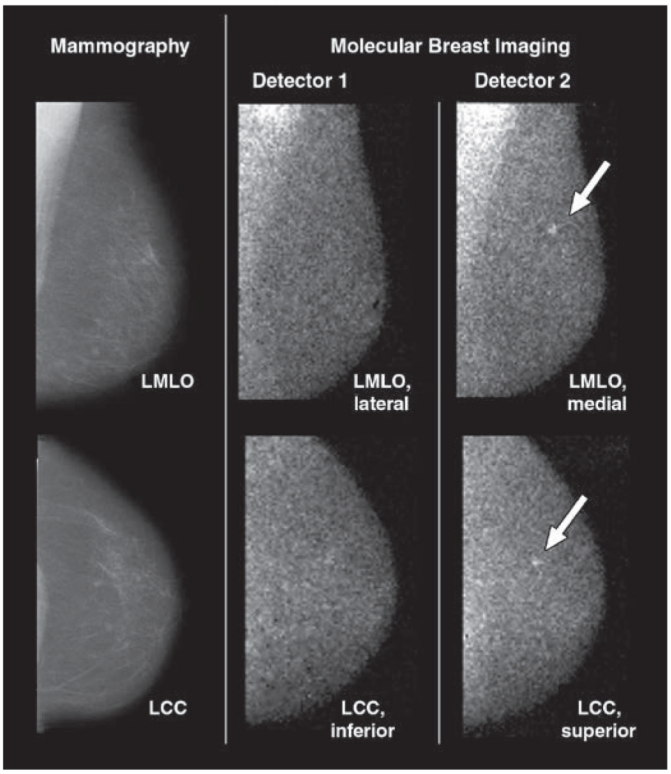

Fig. 5.

82-year-old woman with 4-mm invasive lobular carcinoma (*arrows*) in upper mid left breast at 12-o'clock position 6 cm from nipple. Cancer was initially identified on mammography as BI-RADS category 5 lesion; 5-mm benign intramammary lymph node in lower inner breast was also identified on mammography and sonography. Screening mammograms and craniocaudal and mediolateral oblique views from both molecular breast imaging detectors are shown. During blinded readings of only inferior and lateral molecular breast imaging views from detector 1 (*middle images*), molecular breast imaging findings were interpreted as negative. When superior and medial views from detector 2 (*right images*) were available for molecular breast imaging interpretation in addition to detector 1 views, cancer was identified and given uptake score of 4 (strong focal uptake) by two readers and score of 3 (moderate focal uptake) by third reader. Findings were otherwise negative on molecular breast imaging. LMLO = left mediolateral oblique, LCC = left craniocaudal.

TABLE 1

Sensitivity of Molecular Breast Imaging as a Function of Tumor Histopathology for Each of Three Blinded Readers

Histopathology	No. of Tumors	Reader 1			Reader 2			Reader 3		
		TP	FN	Sensitivity (%)	TP	FN	Sensitivity (%)	TP	FN	Sensitivity (%)
IDC	45	41	4	91	39	6	87	37	8	82
DCIS	17	16	1	94	17	0	100	16	1	94
Mixed IDC and DCIS	29	29	0	100	29	0	100	27	2	93
ILC	21	17	4	81	18	3	86	17	4	81
Mixed IDC and ILC	11	10	1	91	10	1	91	10	1	91
Tubular carcinoma	2	1	1	50	1	1	50	1	1	50
Medullary carcinoma	1	1	0	100	1	0	100	1	0	100
Metaplastic carcinoma	1	1	0	100	1	0	100	1	0	100
Malignant phyllodes tumor	1	1	0	100	1	0	100	1	0	100
Total	128	117	11	91	117	11	91	111	17	87

Note—A total of 128 tumors were present in 88 patients with breast cancer. TP = true-positive, FN = false-negative, IDC = invasive ductal carcinoma, DCIS = ductal carcinoma in situ, ILC = invasive lobular carcinoma.

TABLE 2

Sensitivity of Molecular Breast Imaging as a Function of Tumor Size and Detector Heads Viewed During Blinded Review by Three Readers

Tumor Diameter (mm)	No. of Tumors	Detector Head(s) Used	Reader 1			Reader 2			Reader 3			Average Sensitivity (%)	*p*
			No. of Tumors		Sensitivity (%)	No. of Tumors		Sensitivity (%)	No. of Tumors		Sensitivity (%)		
			TP	FN		TP	FN		TP	FN			
0–5	16	Single	7	9	44	7	9	44	7	9	44	44	0.130
		Dual	11	5	69	11	5	69	10	6	63	67	
6–10	45	Single	31	14	69	39	6	87	33	12	73	76	0.060
		Dual	41	4	91	41	4	91	36	9	80	87	
11–15	30	Single	28	2	93	29	1	97	28	2	93	94	1.00
		Dual	29	1	97	29	1	97	29	1	97	97	
16–20	19	Single	16	3	84	16	3	84	16	3	84	84	0.50
		Dual	18	1	95	18	1	95	18	1	95	95	
> 20	18	Single	16	2	89	17	1	94	17	1	94	92	1.00
		Dual	18	0	100	18	0	100	18	0	100	100	
All tumors ≤ 10	61	Single	38	23	62	46	15	75	40	21	66	68	**0.004**
		Dual	52	9	85	52	9	85	46	15	75	82	
All tumors	128	Single	98	30	77	108	20	84	101	27	79	80	< **0.0005**
		Dual	117	11	91	117	11	91	111	17	87	90	

Note—Difference in the average sensitivity of dual-head molecular breast imaging compared with single-head molecular breast imaging was statistically significant using the McNemar test. **Boldface** indicates statistical significance. TP = true-positive, FN = false-negative.

AJR Am J Roentgenol. Author manuscript; available in PMC 2014 January 08.

TABLE 3

Properties of Nine Tumors in Eight Patients That Were False-Negative (FN) on Readings by All Three Radiologists

FN Tumor No.	Tumor			CC Breast Thickness (cm)	Count Density Percentile	Mammography Breast Density	Comments
	Type	Grade	Size (mm)				
1	IDC	I	13.5	4.9	77.3	Almost entirely fatty	Inadequate positioning due to kyphotic patient; tumor not in view
2	ILC	II	17.5	6.5	15.7	Heterogeneously dense	Image has low count density; lobular cancer
3a	IDC and ILC	I	4.0	4.0	87.6	Heterogeneously dense	Small low-grade tumor; intense nonmasslike tracer uptake
3b	ILC	III	7.0	3.0	92.6	Heterogeneously dense	Intense nonmasslike tracer uptake
4	IDC	I	3.3	6.0	9.2	Heterogeneously dense	Small, low-grade tumor; image has low count density
5	IDC	II	3.3	6.5	9.0	Scattered fibroglandular densities	Small tumor; image has low count density
6	Tubular carcinoma	II	5.0	7.5	13.1	Almost entirely fatty	Small tumor; image has low count density
7	IDC	II	7.3	7.0	36.6	Scattered fibroglandular densities	Inadequate positioning due to obese patient; tumor not in view
8	ILC	I	7.0	7.5	76.2	Heterogeneously dense	Small low-grade lobular cancer

Note—CC = craniocaudal, IDC = invasive ductal carcinoma, ILC = invasive lobular carcinoma.

TABLE 4

Average Sensitivity from Three Blinded Reviews of Single-Head and Dual-Head Molecular Breast Imaging as a Function of the Location of the Tumor Within the Breast

Tumor Location	No. of Tumors	Single Head			Dual Heads			No. of Additional Tumors Detected with Dual Heads vs. Single Head Only
		TP	FN	Sensitivity (%)	TP	FN	Sensitivity (%)	
Upper outer quadrant	48	41	7	85	45	3	94	4
Upper inner quadrant	23	17	6	74	21	2	91	4
Lower outer quadrant	15	12	3	80	13	2	87	1
Lower inner quadrant	4	2	2	50	2	2	50	0
Superior midline	9	6	3	67	7	2	78	1
Inferior midline	7	6	1	86	7	0	100	1
Medial midline	3	3	0	100	3	0	100	0
Lateral midline	11	9	2	82	10	1	91	1
Subareolar and periareolar	8	6	2	75	7	1	88	1
Total	128	102	26	80	115	13	90	13

Note—With single-head molecular breast imaging, detector 1 was used to image the inferior (in craniocaudal [CC] view) and lateral (in mediolateral oblique [MLO] view) aspects of the breast. With dual-head molecular breast imaging, detector 2 was used in addition to detector 1 to also image the superior (in CC view) and medial (in MLO) view of the breast. TP = true-positive, FN = false-negative.

TABLE 5
Sensitivity of Molecular Breast Imaging as a Function of Views Used for Interpretation

Views Used	Reader 1		Reader 2		Reader 3		Average Sensitivity (%)
	No. of Tumors Detected	Sensitivity (%)	No. of Tumors Detected	Sensitivity (%)	No. of Tumors Detected	Sensitivity (%)	
Single-head CC only	90	70	100	78	96	75	75
Single-head MLO only	89	70	100	78	93	73	73
Dual-head CC	109	85	108	84	105	82	84
Dual-head MLO	109	85	109	85	103	80	84
Single-head CC and MLO	97	76	108	84	101	79	80
Dual-head CC and MLO	117	91	117	91	111	87	90

Note—Total number of tumors present was 128. CC = craniocaudal, MLO = mediolateral oblique.